The spin evolution of accreting and radio pulsars in binary systems

Nielsen, A.B.

CHAPTER 2

The X-ray Pulsar 2A 1822-371 as a Super Eddington source

The low mass X-ray binary 2A 1822-371 is an eclipsing system with an accretion disc corona and with an orbital period of 5.57 hr. The primary is an 0.59 s X-ray pulsar with a proposed strong magnetic field of $10^{10} - 10^{12}$ G. In this chapter we study the spin evolution of the pulsar and constrain the geometry of the system. We find that, contrary to previous claims, a thick corona is not required, and that the system characteristics could be best explained by a thin accretion outflow due to a super-Eddington mass transfer rate and a geometrically thick inner accretion flow. The orbital, spectral and timing observations can be reconciled in this scenario under the assumption that the mass transfer proceeds on a thermal timescale which would make 2A 1822-371 a mildly super-Eddington source viewed at high inclination angles. The timing analysis on 13 years of *RXTE* data show a remarkably stable spin-up that implies that 2A 1822-371 might quickly turn into a millisecond pulsar in the next few thousand years.

A. Bak Nielsen, A. Patruno & Caroline D'Angelo
Based on the paper: 2017, MNRAS, Volume 468, Issue 1, p.824-834.

2.1 Introduction

2A 1822-371 is a persistent eclipsing low mass X-ray binary (LMXB) with a 0.59 s accreting X-ray pulsar (Jonker & van der Klis 2001). The neutron star primary accretes material from a 0.62 $M_\odot$ Roche lobe filling main sequence star (Harlaftis et al. 1997), and the system has a binary orbit of 5.57 hr (Hellier et al. 1990; Parmar et al. 2000; Jonker & van der Klis 2001). White et al. (1981) showed that the partial eclipses of the system are best explained by the presence of an accretion disk corona (ADC). The eclipses are clearly seen because the system is being viewed almost edge on at an inclination angle of 81-84° (Heinz & Nowak 2001; Jonker et al. 2003a; Ji et al. 2011), which was found through modelling of the light curve (Heinz & Nowak 2001). As shown by Heinz & Nowak (2001) the eclipse of 2A 1822-371 is a narrow peak in the light curve, however, most of the light curve, about 80 % of the orbit, is obscured. White & Holt (1982) suggested that the ADC is formed by evaporated material in the inner accretion disc due to radiation pressure from the X-rays produced by the neutron star. The accretion disc is thought to be optically thick and the ADC appears so extended that it is not completely blocked by the companion star. Indeed the companion seems to eclipse about 50% of the total light emitted (Mason & Cordova 1982; Somero et al. 2012). The magnetic field of 2A 1822-371 was inferred twice from the presence of cyclotron resonance scattering features (crsf). Sasano et al. (2014) reported results obtained with *Suzaku* and suggested a crsf at 33 keV which would correspond to a magnetic field of B$\sim 2.8\times10^{12}$ G. This, however, was in disagreement with the later findings of Iaria et al. (2015) who interpreted *XMM-Newton* spectral data as showing a crsf at around 0.7 keV (and an inferred magnetic field of B$\sim 8.8\times10^{10}$ G).

The intrinsic X-ray luminosity (L_X) of 2A 1822-371 is currently not well constrained. The first source of uncertainty comes from the distance, which is not well known although it was estimated to be around 2-2.5 kpc based on modelling of infrared and optical observations (Mason & Cordova 1982).
Mason & Cordova (1982) estimated the luminosity to be $L_X \sim 1.1\times10^{35}\,(d/1kpc)$ which, for a distance of about 2.5 kpc is $\sim10^{36}$ erg s^{-1}. Since the pulsar is seen edge-on, its optical to X-ray luminosity ratio is $L_{\rm opt}/L_X \sim 15-65$. This value is very anomalous among LMXBs, which have a typical ratio of the order of $\sim$1000. The binary also shows a very large orbital period derivative of $\dot{P}_{orb}$=1.5-2.1$\times10^{-10}$ s s^{-1} (implying a very fast orbital expansion Burderi et al. 2010; Jain et al. 2010; Iaria et al. 2015), and thus it has been suggested that the binary is undergoing a highly non-conservative mass transfer, with the neutron star accreting at the Eddignton-limit and the rest of the material expelled from the donor star via radiation pressure (e.g., Iaria et al. 2015). This also suggests the possibility that 2A 1822-371 is an Eddington limited source Jonker et al. (2003a) which would then be compatible with one of the magnetic field estimates inferred from the crsf (i.e., $B = 8.8\times10^{10}$ G). Another peculiar phenomenon in 2A 1822-371 is the fast spin up of the system, which gives an extremely short spin-up timescale of order 7000 yr (Jonker & van der Klis 2001). When looking at the ensemble of slow accreting pulsars in LMXBs, the short spin-up timescale of 2A 1822-371

is not unique. Indeed short timescales have previously been observed in LMXB pulsars such as 4U 1626-67 and GX 1+4, both of which show torque reversals (Bildsten et al. 1997; Jonker & van der Klis 2001). The accretion torque reversal is a still poorly understood phenomenon that occurs in some accreting pulsars and that causes a switch from a spin-up to a spin-down (and vice-versa). One possible interpretation of torque reversals is a transition between a Keplerian and a sub-Keplerian flow in the inner portion of the accretion disk (e.g., Yi et al. 1997).

The spin evolution of 2A 1822-371 can therefore be explained with two different scenarios: either the system has started accreting very recently (if the currently observed spin-up truly represents the secular evolution of the neutron star spin) or, alternatively, what we are observing is simply a short-term effect with the current spin up that will be possibly balanced by an episode of spin-down in the next future. The latter scenario would make 2A 1822-371 similar to the other high field LMXB pulsars like 4U 1626-67 and GX 1+4. In those two systems, the phenomenon of torque reversals occurs on timescales of years. Other pulsars, such as Her X-1, Cen X-3 and Vela X-1 (the latter two are high mass X-ray binaries) show variations on shorter timescales of days to a few years (see for example Fig. 6 in Bildsten et al. (1997)). Since several other LMXB pulsars show changes in their spin frequency derivative, we investigate here whether long-term spin-up in 2A 1822-371 is really stable or if there are underlying detectable fluctuations related to accretion torque variations.

A second problem is that, at least in the (low magnetic field) accreting millisecond pulsars, measuring the spin frequency derivative is sometimes complicated by the presence of timing noise in the X-ray time of arrivals of pulsations (Hartman et al. 2008; Patruno et al. 2009). It has, however, been observed that at least in some accreting millisecond pulsars, a large part of timing noise is correlated to variations in flux (Patruno et al. 2009, 2010; Haskell & Patruno 2011). One plausible interpretation of the flux-phase correlation is that the hot spot is moving on the pulsar surface in response to variations of the mass accretion rate. In high field accreting pulsars like 2A 1822-371 the presence of such correlation has never been reported and it is currently unclear whether such effects might be present in these systems too. For example, the stronger magnetic field of the neutron star in 2A 1822-371 might prevent a drift of the hot spot when the accretion rate varies. However, strong timing noise has been observed in the accreting X-ray pulsar Terzan 5 X-2 (Patruno et al. 2012a), which is an 11 Hz accreting pulsar with a magnetic field of the order of $10^9 - 10^{10}$ G, which is substantially stronger than the typical field observed in accreting ms pulsars ($B \sim 10^8$ G). Therefore it might be possible that the same phenomenon is present in 2A 1822-371 and in this work we plan to investigate this. There are therefore two questions that need to be addressed for 2A 1822-371:

1. Is the previously measured spin frequency derivative the true one or its measurement is affected by the presence of timing noise?

2. Does the (true) spin frequency derivative represent the long term spin evo-

lution of the neutron star?

In this chapter we use archival data from the *Rossi X-ray Timing Explorer* (*RXTE*), collected over a baseline of 13 years, to try to answer the aforementioned questions.

Furthermore, it has been suggested that the ADC forms an optically thick region around the neutron star (White & Holt 1982; Parmar et al. 2000; Iaria et al. 2001), with optical depth $\tau \sim 9 - 26$, which implies that most of the light coming from the pulsar is heavily scattered. However, at such large optical depths the coherent pulsations cannot preserve their coherence. Iaria et al. (2013) first noticed this problem and suggested that the Comptonised component is produced in the inner regions of the system which are never directly observed. Then only a small fraction ($\sim 1\%$) of the total light produced is scattered along the line of sight of the observer with an optical depth $\tau \sim 0.01$. This geometry, although possible, requires some fine tuning of the optical depth. Furthermore, to preserve the coherence of the pulsations, the whole (optically thick) Comptonization region needs to rotate with the neutron star. A third question that needs to be answered is therefore whether it is possible to keep a simple geometry of the system, with an ADC, and still obtain a spectrum compatible with $\tau \sim 1$.

In section 2.2 we present the observations and the data reduction procedure, in section 2.3 we show our results on the timing analysis, e.g. the spin evolution and flux-phase correlation, and in section 2.4 we discuss the implications of our finding and we extend previous models for 2A 1822-371 .

2.2 X-Ray Observations

We have used data taken over a baseline of 13 years, between 28 June 1998 and 30 November 2011. All observations were taken with the Proportional Counter Array (PCA) on board the *RXTE* (Bradt et al. 1993; Jonker & van der Klis 2001). *RXTE*/PCA consists of five xenon/methane proportional counter units, which are sensitive in the range of 2-60 keV (Jahoda et al. 2006). We chose science event files with a time resolution of 2^{-16}s (Event_16us), 2^{-13}s (Event_125us) and 2^{-20}s (GoodXenon) for the timing analysis whereas we selected Standard 2 data with 16 s time resolution to construct the X-ray lightcurve. The lightcurve is reconstructed in the 2–16 keV energy range and the X-ray flux is first averaged for each observation (ObsID) and then normalized in Crab units (see Fig. 2.4). A detailed description of this standard procedure can be found in van Straaten et al. (2003). The timing analysis is performed by selecting the absolute energy channels 24 to 67 that correspond approximately to an energy range of ≈9-23 keV. This range was chosen because the pulsation have the highest signal to noise ratio (S/N) as reported by Jonker & van der Klis (2001). The data was barycentered with the FTOOL *faxbary* by using the JPL DE405 Solar System coordinates and the most precise astrometric position found by *Chandra* observations, RA: 18:25:46.81 and DEC: -37:06:18.5 (Burderi et al. 2010) with an error of 0.6" (90% uncertainty circle of the *Chandra* X-ray absolute position). The barycentered data was then epoch folded in pulse profiles of 32 bins over either 1500 s, or the total length of the

data segment, which usually corresponds to 3000 s. We then cross-correlated each pulsation with a sinusoid at the spin frequency of the pulsar and generated a set of time of arrivals (TOAs). We selected only pulsations with a S/N larger than 3.1σ, defined as the ratio between the pulse amplitude and its 1 sigma statistical error. The value of 3.1σ is selected to account for the number of trials, i.e., we expect less than 1 false pulse detections among the 281 pulse profiles generated over the entire 13 year baseline. We looked for the presence of a 2^{nd} harmonic which was detected only is a small subset of data segments and thus we do not consider it any further in the forthcoming timing analysis.

The ephemeris used in the epoch folding are composed by an initial pulse frequency from Jonker & van der Klis 2001 and Jain et al. 2010 and an orbital solution from Iaria et al. 2011. The orbital solution corresponds to a Keplerian circular orbit with a constant orbital period derivative. Since the data contains large data gaps we split it in 20 segments that could be potentially phase connected, meaning that our time baseline for each different segment spans typically a few days, see table 2.1. With the S/N criterion discussed above, we found significant pulsations in 15 out of 20 data segments. In this work we have used TEMPO2 version 2012.6.1 and kept the orbital values fixed throughout the analysis.

2.3 Results

Pulsations are found in the first 15 data segments described in table 2.1. In the last 5 data segments the S/N found was lower than the selected 3.1σ for most of the pulsations, thus leaving us with too few or no pulsations to perform the timing analysis. In table 2.1 we provide the 95% confidence upper limit of the fractional amplitude of the pulsations in these 5 data segments. All these upper limits are consistent with the fractional amplitude found in the first 15 data segments.

2.3.1 Spin Evolution

In two out of fifteen data segments the pulse time of arrivals of the neutron star required a spin frequency derivative. The χ^2 and degrees of freedom (dof) for the fits to all 15 data segments are given in table 2.1. The errors on the spin frequency were calculated by using standard χ^2 minimization techniques and by multiplying them by the square root of the reduced χ^2. The errors on the spin period is found from: $\sigma_P{=}\sigma_\nu(\frac{1}{\nu})^2$.

The collection of all spin frequencies (see Table 2.1) is then fitted with a linear function to determine the long-term spin frequency derivative over the entire baseline of the observations. The fit gives a reduced χ^2 of 1909 for 11 dof. This indicates that the fit is not statistically acceptable (p-value$<0.05\%$) and the bad fit is caused by several points that are clearly off the linear relation (see lower panel of Fig. 2.1). The best-fit linear slope that we find corresponds to a spin up of $\dot{\nu}{=}7.6(8){\times}10^{-12}\,\mathrm{Hz\,s^{-1}}$ for the period ranging from June 1998 to November 2011, comparable to what has recently been found by Chou et al. (2016).

The bad fit to the spin frequencies shows that, although there is no evidence

Table 2.1: Overview of the data used throughout this chapter. The data are taken with *RXTE*, and in this data, segments 3, 9, 10, 13, 14, 15 represent data not analysed before in the literature Jain et al. (2010); Somero et al. (2012); Jonker & van der Klis (2001). The errors reported in the parentheses correspond to 1σ statistical errors. The χ^2 and dof given in the table is for the TEMPO2 spin frequency fit to the data. The 95% upper confidence limit is only given for the data segments were there were not found any significant pulsations (significance limit was 3.3σ).

#	ObsId	T_{start}	T_{end}	Upper limit (%)	PEPOCH	Spin frequency (ν_0)	Spin period (P_s)	χ^2	dof
1	30060	50992.8210	50993.9805		50993.1873	1.6860862(6)	0.59308949(2)	28.49	6
2	30060	51018.2434	51019.6464		51018.9449	1.6860957(3)	0.59308615(9)	63.30	17
3	50048	52031.5426	52032.8178		52032.1105	1.6866984(4)	0.5928742(3)	35.43	13
4	50048	52091.4522	52101.4647		52096.4049	1.6867365(2)	0.59286083(7)	47.41	12
5	70036	52435.4107	52435.7670		52435.5174	1.686932(2)	0.59279212(5)	25.54	8
6	70037	52488.3701	52495.9115		52491.9201	1.68697104(4)	0.5927784(2)	100.13	26
7	70037	52503.3513	52503.9363		52503.5256	1.686980(2)	0.59277526(5)	21.77	8
8	70037	52519.1659	52519.5110		52519.3091	1.686988(4)	0.59277244(1)	42.79	6
9	70037	52547.3079	52547.8544		52547.3944	1.6870063(10)	0.59276601(4)	26.31	9
10	70037	52608.1849	52608.3845		52608.2072	1.686879(8)	0.59281075(3)	11.22	2
11	70037	52882.0214	52882.2226		52882.3290	1.687240(4)	0.59268391(2)	8.81	3
12	70037	52883.1514	52885.1249		52883.4896	1.6869901(8)	0.59277171(3)	20.55	2
13	80105	52896.2822	52896.4384		52896.2556	1.687243(3)	0.59268286(9)	11.12	4
14	96344	55880.6677	55884.8487		55882.5852	1.6891897(2)	0.59199982(6)	85.27	17
15	96344	55888.5020	55895.6318		55891.8696	1.68920448(8)	0.59199464(3)	23.85	7
16	60042	52138.7535	52141.8115	2.1	-	-	-	-	-
17	60042	52138.7535	52141.8115	2.1	-	-	-	-	-
18	50048	51975.7203	51976.1843	0.7	-	-	-	-	-
19	70037	52432.3887	52432.7906	0.6	-	-	-	-	-
20	70037	52724.7351	52724.7545	0.5	-	-	-	-	-

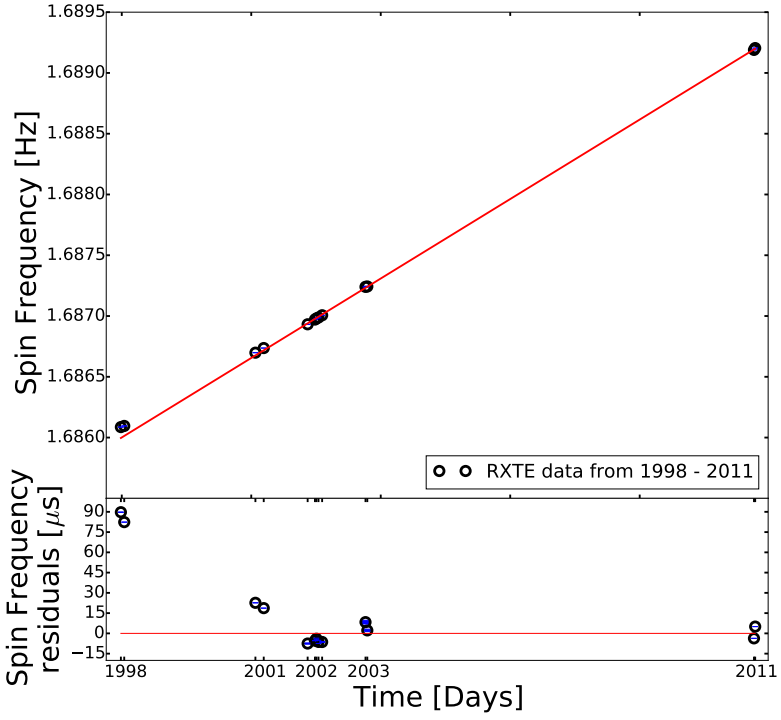

Figure 2.1: The longterm spin up over a time period of 13 years. The black points show the data used in this chapter and listed in table 2.1. The red line is a fit to the data from this chapter and it gives the spin up of the pulsar of $\dot{\nu}$=7.57(6)$\times 10^{-12}\,\mathrm{Hz\,s^{-1}}$. This figure is plotted with errors on all points, seen in blue. Most of the errors are, however, so small that they are not visible on the plot.

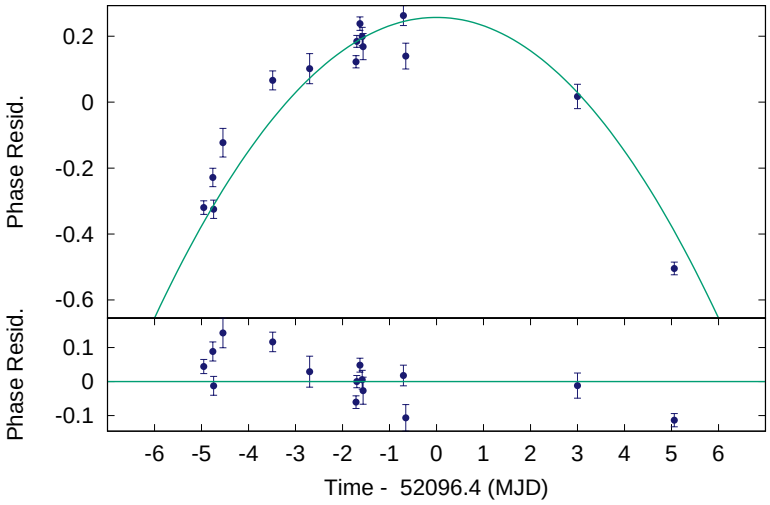

Figure 2.2: The pulse phase residuals before a spin frequency derivative is fitted for (top panel) and after (lower panel). The parabola is a clear evidence of the presence of a spin frequency derivative.

for a change in sign of the spin frequency derivative, some fluctuations are present in the data. We thus explored to what extent the magnitude of the accretion torque vary with time and whether *small/short-term* torque reversals are present in the data. First, in the data segments 4 and 6, it was possible to phase-connect the pulsations and we thus have a direct measure of the spin frequency derivative. Such spin frequency derivative is measured for a time interval of 10 and 8 days (for segment 4 and 6, respectively). The two spin up values found are $\dot{\nu}$=6.7(4)$\times 10^{-12}$ Hz s^{-1} for segment 4 and $\dot{\nu}$=8.2(5)$\times 10^{-12}$ Hz s^{-1} for segment 6 which are both within 1σ from the long-term linear trend seen in the 13-year long baseline.

The pulse phase residuals with respect to a constant spin frequency model can be seen for the data segment 4 in the top panel of Fig. 2.2. In the lower panel of the same figure we show the pulse phase residuals with respect to a spin frequency derivative model. The parabolic trend seen in the top panel of Fig. 2.2 is a clear signature of the presence of a frequency derivative.

2.3.2 Spin period derivative vs. time

To estimate the magnitude of the spin fluctuations we calculated the spin period derivative between each consecutive data point, i.e., we determined the slope between each pair of points, and plotted them versus time, see Fig. 2.3. The errors

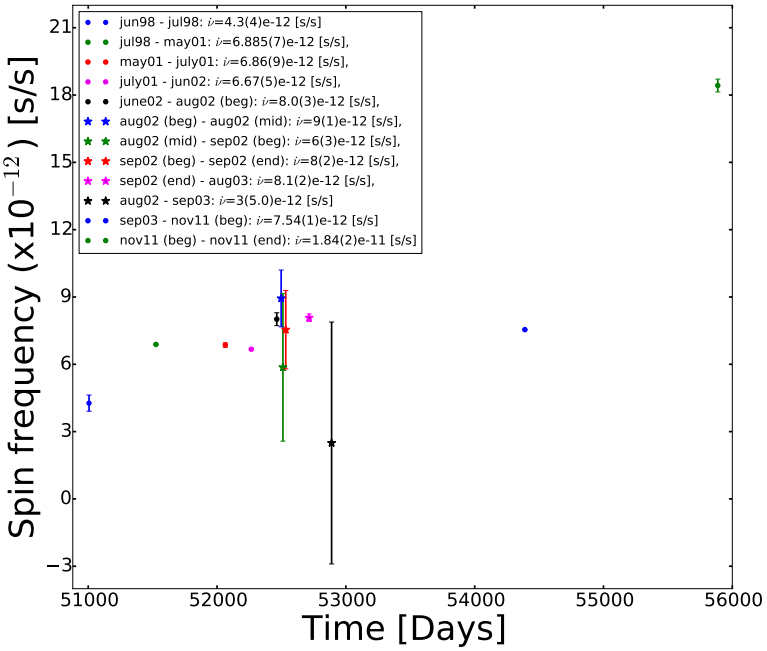

Figure 2.3: The spin period derivative change between the individual observations from Fig. 2.1. It is clearly seen that most of the observations coincide, and there is a close to constant development in the spin period derivative. However, there are a few points that are off, e.g. in 2003 and 2011.

on the spin period derivatives are found by taking the maximum and minium slope between the spin periods in Fig. 2.1. It is clear that most of the points in Fig. 2.3 are roughly consistent with a single constant spin period derivative with small variation of less than a factor 2 over the whole baseline with the exception of an outlier in the last data segment taken in 2011. In that case the spin frequency derivative is consistent with having increased by a factor 3 during the last month of the observations.

The 2–16 keV X-ray flux shows a variation of less than a factor 2 during that same month (see Figure 2.4) and no average variation when compared to the average X-ray luminosity of the previous years.

2.3.3 X-Ray Flux-Phase Correlation

2A 1822-371 is a persistent source that shows little variability in X-ray flux. In all our observations the X-ray flux varies by less than a factor of 2 with respect to the average value. Therefore even if a flux-phase correlation is present in 2A 1822-371 we expect little or no variation in the X-ray pulse phases. Nonetheless we inspected the data for the presence of such correlation, since it is the first time

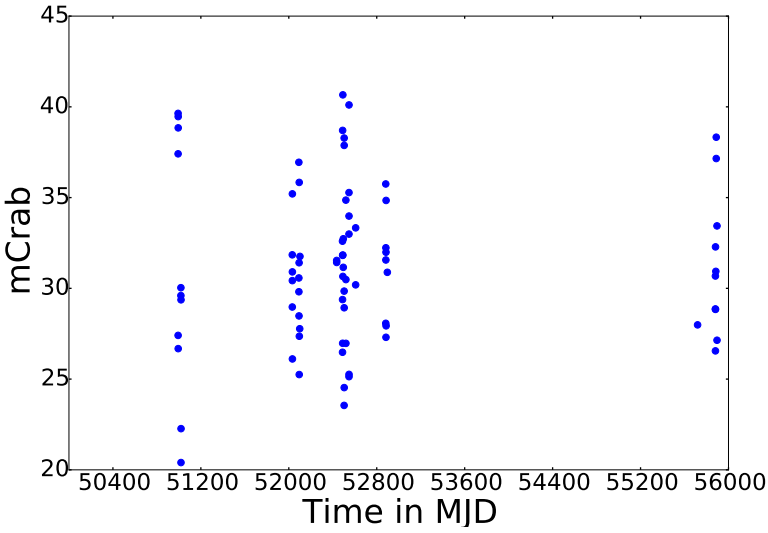

Figure 2.4: 2–16 keV X-ray lightcurve of 2A 1822-371. Each data point represents an ObsID average flux. The overall intensity of the light curve is fairly constant over the span of the observations used in this chapter, with variations of less than a factor 2 in 13 years of observations.

that such a test is performed in such a high field accreting pulsar.

We follow the procedure outlined in Patruno et al. (2009, 2010) i.e., we minimize the χ^2 of a linear fit to the X-ray flux vs. pulse phase. If there is a significant correlation then this might indicate the existence of some mechanism that determines the pulse phase variations in addition to genuine neutron star spin variations. Such mechanism for example can be the motion of the hot spot on the surface of the pulsar (Patruno et al. 2009, 2010).

We fit the data with a linear correlation

$$\phi = a + b\,F_x \tag{2.1}$$

where ϕ is the pulse phase and F_x the X-ray flux. If there is a correlation, b should be significantly different than zero. However, in all our 15 data segments, the b coefficient is consistent with zero within the statistical errors as can be seen in table 2.2.

2.3.4 Fractional Amplitude vs. cycles

We tested whether there was a correlation between the fractional amplitude of the pulsations and the eclipses with the purpose of testing whether we can actually directly see the surface of the neutron star when there is no eclipse.

On Fig. 2.5 we report the results of the data analyzed from 2002 and 2011. The fractional amplitude definition is the same as the one used in Patruno et al. (2010). When pulsations are not detected we provide 95% confidence level upper

Table 2.2: The A and B value for the Flux-Phase correlation fits for the individual data segments.

# segment	a	b
1	-0.08(10)	0.001(2)
2	0.20(3)	-0.0087(7)
3	0.2(1)	-0.007(4)
4	0.81(6)	-0.03(2)
5	0.08(7)	-0.003(2)
6	0.004(40)	-0.0001(15)
7	0.19(5)	-0.008(2)
8	-0.22(5)	0.010(2)
9	0.12(5)	-0.005(2)
10	-0.5(1)	0.019(4)
11	-1.8(2)	0.080(7)
12	0.11(8)	-0.004(3)
13	0.4(1)	-0.012(3)
14	-0.07(5)	0.002(2)
15	-1.20(7)	0.033(2)

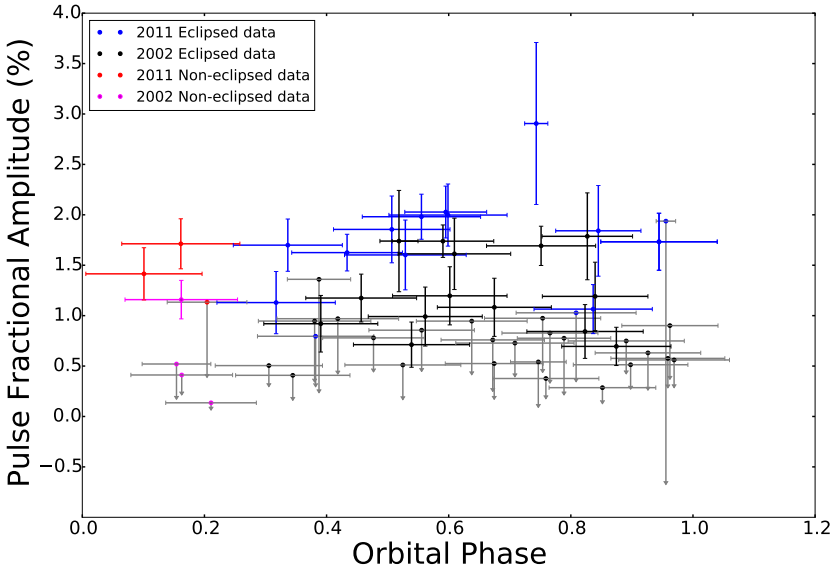

Figure 2.5: The fractional amplitude of eclipsed data and the non-eclipsed data vs. the cycle of the pulsar. The Eclipse fractional amplitudes are seen in blue/black (2011 and 2002 data), and the non-eclipsed fractional amplitudes are seen in red/pink (2011 and 2002). The non-eclipsed data is assumed to be 0.05-0.25 cycle, and the rest of the cycle is assumed to be a part of the eclipse. The eclipse is defined with a zero point at T_{ASC}.

limits. The red and pink points on Fig. 2.5 are the data from the non-eclipsed part of the lightcurve, and the blue and black points are from the eclipsed part of the orbit. We use T_{asc} as our reference orbital phase zero (i.e., the beginning of the cycle) and we thus expect that the non eclipsed data are between cycle 0.05-0.25. We further use the fact that the rest of the cycle is partially eclipsed. Note some other authors use a different definition of eclipse, for example Heinz & Nowak (2001), define the eclipse to be only the portion of the lightcurve that shows a deep dip (Hellier et al. 1990; Heinz & Nowak 2001). In any case, Fig. 2.5 shows that there is no detectable difference between the fractional amplitudes for the eclipsed and non eclipsed data in any orbital phase interval.

2.4 Discussion

In this chapter we have found a long-term spin frequency derivative of $\dot{\nu}$=7.6(8)$\times 10^{-12}\,\mathrm{Hz\,s^{-1}}$, and a short term spin frequency derivative of $\dot{\nu}$=(6–8)$\times 10^{-12}\,\mathrm{Hz\,s^{-1}}$, in two phase connected data segments. The long-term spin up is consistent with that reported by Chou et al. (2016), Iaria et al. (2015), Jain et al. (2010) and Jonker & van der Klis (2001). We find no evidence for torque reversals and few variations in the accretion torque, limited to fluctuations of less than a factor two with the exception of the last data segment in 2011, where the spin up requires an increases by a factor 3 with respect to the overall long-term spin frequency derivative. There is no corresponding increase in the X-ray flux (in the 2–16 keV band) at the time of the spin-up increase. Finally, no evidence for a phase-flux correlation and no strong variations in the X-ray flux of the source are found.

Previous papers have suggested different models and parameters for 2A 1822-371. A summary of some of the most recent papers is found in table 2.3. The data examined in this chapter span a baseline of about 13 years, from 1998 to 2011. In the following sections we will try to explain the long-term spin evolution with a self consistent model that can explain the measured strength of the magnetic field, the neutron star spin frequency derivative and the mass transfer rate. Then we will move on to comment on the different possible magnetic fields reported by Iaria et al. (2015) and Sasano et al. (2014). We then proceed to discuss whether the observed spin frequency derivative reflects a secular spin up that will continue in the future, or whether we are indeed just observing a short-term spin up that will change sign and or magnitude in the future.

2.4.1 Long term spin evolution

The large spin up of 2A 1822-371 implies a very short spin-up time scale of about $\nu/\dot{\nu} \approx 7000\,\mathrm{yr}$. This is an extremely short time scale for a system that should take several million years to spin up (Bhattacharya & van den Heuvel 1991). The relatively constant spin up implies no variation in the accretion torques acting upon the neutron star at least down to timescales of 8-10 days. However, as shown in Section 2.3.1 the linear fit to the spin frequency vs. time gives a very large χ^2

which implies that the spin frequency is not increasing linearly with time. This would be expected in case of constant accretion torque, but the observed flux has an rms fluctuation of the order of 4.4 mCrab, suggesting that accretion torques do indeed vary slightly with time. The strongest evidence for this comes from the last data point in 2011 where the spin up increase by a factor 3. Accretion theory predicts that the strenght of the spin up should scale with the amount of mass accreted according to the following relation (see e.g., Bildsten et al. 1997):

$$\dot{\nu} \propto \dot{M}^{6/7}. \tag{2.2}$$

If the mass accretion rate is related to the X-ray luminosity (and thus the X-ray flux) with the usual relation $L_X \approx \eta\, c^2 \dot{M}$ then we should expect $\dot{\nu} \propto F_X^{6/7}$. Therefore a $3\times$ larger $\dot{\nu}$ should imply a $\approx 3\times$ larger X-ray flux. However, the average 2–16 keV X-ray flux is not varying, on average, by this amount and therefore this probably means that the 2–16 keV X-ray flux is not a good tracer of the instantaneous mass accretion rate. Such possibility has been proposed to explain the behaviour of a number of other LMXBs (van der Klis 2001).

We now wish to test if we can find a self consistent model that explains the observed spin parameters of 2A 1822-371. First, let's define the co-rotation radius as that point in the accretion disk where matter has the same angular velocity of the neutron star:

$$R_{CO} = \left(\frac{GM_{NS}}{4\pi^2 \nu^2} \right)^{1/3} \tag{2.3}$$

Then, following Ghosh & Lamb (1979), we can define the magnetospheric radius as the point where the ram pressure of the disk plasma equals the magnetic pressure:

$$R_m = \xi R_A = \xi \left(\frac{\mu^4}{2GM_{NS}\dot{M}^2} \right)^{1/7} \tag{2.4}$$

Such definition has some issues since it is derived by equating the dipolar magnetic field pressure to the ram pressure of a spherically symmetric free falling gas. The factor $\xi \approx 0.5$ is typically used to account for the disk geometry instead of the spherical symmetry of the free falling gas. Several works (Aly 1985; Lovelace et al. 1995, Goodson et al. 1997) have demonstrated that the magnetospheric-disk interaction will quickly generate an azimuthal field component that causes many field lines to open and reconnect at infinity. D'Angelo & Spruit (2010, 2012) have thus derived a different version of the magnetospheric radius which accounts for this differences. The magnetospheric radius thus obtained however, is not substantially different from the expression above and since we are giving only an order of magnitude estimate of the quantities we will continue to use the definition above. This makes also the comparison with other works more direct, since they mostly rely on the definition of magnetospheric radius given by Ghosh & Lamb (1979)

From the table 2.3, we can see that a few parameters reported in the literature (e.g., B, L_x, $\dot{P}_s$, etc.) are not consistent with each other and sometimes some reported values are even inconsistent from a physical point of view. For example,

Table 2.3: The different parameters in the most recent published papers on 2A 1822371. The papers are JvdK2001 = Jonker & van der Klis (2001), Jain2010=Jain et al. (2010),BU2010=Burderi et al. (2010), Bay2010=Bayless et al. (2010), Ia2011= =Ialria et al. (2011), Som2012=Somero et al. (2012), Sas2014=Sasano et al. (2014) & Ia2015=Ialria et al. (2015)

Parameter	JvdK2001	Jain2010	Bay2010(UV/Optical)	Sas2014	Ia2015
$\dot{\nu}$ (Hz/s)	$(8.1\pm0.1)\times10^{-12}$	$(7.06\pm0.01)\times10^{-12}$	-	$(6.9\pm0.1)\times10^{-12}$	$(7.25\pm0.08)\times10^{-12}$
$\dot{P}_{Spin}$ (s/s)	$-2.85(4)\times10^{-12}$	$-2.481(4)\times10^{-12}$	-	$-2.43(5)\times10^{-12}$	$-2.55(3)\times10^{-12}$
L_X (erg/s)	10^{36}-10^{38}	$(2.38\text{-}2.96)\times10^{38}$	$\sim10^{37}$	$\sim10^{37}$	1.26×10^{38}
$\dot{M}(M_\odot/yr)$	-	$(4.2\text{-}5.2)\times10^{-8}$	6.4×10^{-8}	-	-
$M_{NS}(M_\odot)$	1.4	1.4	1.35	1.4	1.61-2.32
B (G)	10^{8}-10^{16}	$(1\text{-}3)\times10^{8}$	-	2.8×10^{12}	$8.8(3)\times10^{10}$
Pulse Amp	0.25-3%	-	-	$\sim \pm5\%$	$\sim$0.75%
$P_{orb}/\dot{P}_{orb}$ (yr)	-	$(4.9\pm1.1)\times10^{6}$	$(3.0\pm0.3)\times10^{6}$	-	-
P_s (s)	0.59325(2)	0.5926852(21)	-	0.592437(1)	0.5928850(6)
Time span	1996-1998	1998-2007	1979-2006	2006	1996-2006

magnetic field strengths as large as 10^{16} G have been discussed by Jonker & van der Klis (2001), by using the relation between B and μ, which, can only be used when $R_m < R_{CO}$, since there will be no accretion if the magnetospheric radius is outside of the co-rotation radius (with the exception of accretion induced by magnetic diffusivity, see e.g.,Ustyugova et al. (2006)). For 2A 1822-371, the co-rotation radius is at $\approx$ 1200 km, so that any magnetospheric radius larger than this value cannot be inferred by using Eq. 2.3. With a B field of 10^{16}G one would indeed obtain a magnetospheric radius of 10^6 km for a luminosity of 10^{36}erg s^{-1}.

Since we know $\dot{\nu}$ we can use the relation for the X-ray luminosity to find the mass accretion rate ($\dot{M}$) (Frank et al. 2002):

$$\dot{M} = \frac{L_X R_{NS}}{G M_{NS}} \tag{2.5}$$

This assumes that the X-ray luminosity does trace the instantaneous mass accretion rate, which is, however, not the case in 2A 1822-371 as we have shown above. To obtain an expression for μ that we have used in Eq. 2.4 we use the angular acceleration as a function of $\dot{M}$, $\dot{\Omega} = 2\pi\dot{\nu} = \frac{\dot{M}\sqrt{G M_{NS} R_m}}{I}$ which gives:

$$\dot{\nu} \approx 4.1 \times 10^{-5} \dot{M}\, M_{NS}^{1/2}\, R_m^{1/2}\, I^{-1} \mathrm{Hz/s}. \tag{2.6}$$

In the above equation we use the measured long-term $\dot{\nu}$, and we assume a neutron star mass of 1.4 $M_\odot$, a neutron star radius of 10 km, the moment of inertia ($I = 10^{45}$ g cm^2, ξ=0.5. We assume 1.4 $M_\odot$ in the above, even though Iaria et al. (2015) find the mass of the neutron star to be (1.69$\pm$0.13) $M_\odot$ and find the companion mass to be (0.46$\pm$0.02) $M_\odot$, within the limits given by Muñoz-Darias et al. (2005).

We can see that the models that satisfy the condition $R_m < R_{CO}$ are those where the luminosity is in excess of the Eddington limit. However, it is not known if the star really does accrete at near the Eddington limit. The observed X-ray luminosity is only $L_X \approx 10^{36} (d_2)^2$erg s^{-1} assuming a (poorly constrained) distance of 2 kpc. The best distance approximation is between 1-5 kpc (Mason & Cordova 1982; Parmar et al. 2000) which however, would shift the luminosity by less than an order of magnitude. The most compelling evidence that the X-ray luminosity is indeed higher than the observed value is that the ratio L_x/L_{opt} $\approx$15-65 and not 500-1000 as observed in other LMXBs (Griffiths et al. 1978; Bayless et al. 2010; Somero et al. 2012; Iaria et al. 2015). This means that either the optical luminosity is much larger than expected or that only a small $(1 - 10\%)$ of the total X-ray luminosity of the source is effectively observed.

A source accreting at the Eddington rate requires a mass accretion rate of $\dot{M} \sim 10^{-8} M_\odot$/yr. This is 2 orders of magnitude larger than what is expected from binary evolution models under the assumption that the donor is a main sequence star that started Roche lobe overflow with a mass $\lesssim 1\, M_\odot$ and that the binary evolution is driven by angular momentum loss via magnetic braking (Podsiadlowski et al. 2002). Since 2A 1822-371 is a persistent source, the mass accretion rate (from the disk to the neutron star) must be equal (or very close to) the mass transfer

rate (from the donor to the accretion disk). Therefore in this model the system will only survive for about 1 Myr.

It is interesting to compare the behaviour of 2A 1822-371 with that of Terzan 5 X-2, another pulsar that is in many ways similar to 2A 1822-371. Terzan 5 X-2 is an 11 Hz accreting pulsar which is accreting from a sub-giant companion ($M \gtrsim 0.4\,M_{\odot}$) in a relatively large orbit (orbital period of 21 hr). The neutron star has a dipolar magnetic moment in the range of $\mu \simeq 10^{27}$-$10^{28}\,\mathrm{G\,cm^3}$ (Cavecchi et al. 2011; Papitto et al. 2011; Patruno et al. 2012b). This system has a clear spin-up of $\dot{\nu} \sim 10^{-12}\,\mathrm{Hz\,s^{-1}}$, and it appears to be evolving towards a millisecond pulsar in a very short timecale of a few tens of million years (Patruno et al. 2012b). Both 2A 1822-371 and Terzan 5 X-2 seem to be at odd with the very long phases that binaries with similar spin and orbital parameters spend in Roche lobe contact, which can last for about 1 Gyr or more. (Patruno et al. 2012b) proposed that Terzan 5 X-2 is in an exceptionally early RLOF phase although the reason why we are witnessing this unlikely event remains an open problem. Indeed observing two pulsars being recycled in an early RLOF phase in the relatively small population of LMXBs is unlikely. This means that the exceptionality of Terzan 5 X-2 cannot be due to chance alone and there must be a common evolutionary process that creates this kind of accreting pulsars. By using the proper motion, the radial velocity and the current position of 2A 1822-371, it is possible to find the original position and give an estimate of the age of the system. Maccarone et al. (2014) found 2A 1822-371 to likely originate from close to the Galactic center, and reported an age of about 3–4 Myr, which indeed makes the system very young (Maccarone et al. 2014) (although there is a quite big uncertainty due to the poorly constrained distance of the system). This may support the analogy that the system is similar to Terzan 5 X-2 and they both are in an early Roche lobe overflow phase.

2.4.2 Torque reversal

2A 1822-371 share a few common features with other accreting pulsars, besides Terzan 5 X-2. Short spin-up time scales are seen also in the ultra-compact binary 4U 1626-67 (Chakrabarty et al. 1997) which has $\nu/\dot{\nu}$=5,000 yr (Chakrabarty et al. 1997; Beri et al. 2014). 4U 1626-67 is a quite different binary from 2A 1822-371 since it is an ultra compact system ($P_{\mathrm{orb}} \approx 42$ min), the companion star is not a main sequence star, but rather a degenerate He or CO white dwarf, and the neutron star has a spin of 7.66 s. The system was originally discovered in 1972 by Giacconi et al. (1972). Torque reversal of the system was observed for the first time in 1990, where the system was found to be spinning down rather than up, as previously observed (Chakrabarty et al. 1997; Beri et al. 2014).

The torque reversal phenomenon is not very well understood since it is unclear what its origin is and what triggers it. However, the accretion torque in 4U 1626-67, no matter the sign of the spin frequency derivative, is very steady on timescales of years, which means that the accretion is almost certainly from an accretion disk. Chakrabarty et al. (1997) even found that the pulsar seems to be accreting steadily during spin-down. The first phase of spin-up lasted for at least 13 yr, the spin-down then lasted about 18 yr, and in 2008 4U 1626-67 began spinning up again

(Beri et al. 2014). In 4U 1626-67 the torque reversals are accompanied by sudden variations in the X-ray luminosity (Chakrabarty et al. 1997). A decrease in X-ray flux was seen when the neutron star moved from a spin-up to spin-down phase, and again there was an increase by a factor 2 in the X-ray flux with the second torque reversal (Beri et al. 2014). The very short spin-up timescale found for 2A 1822-371 is thus not incompatible with the notion that this system too will show a torque reversal somewhere in the near future.

2.4.3 Accretion Disc Corona

From the spectral analysis of 2A 1822-371 and from the shape of the eclipses it is evident that there is some extended X-ray emitting region around the pulsar, often assumed to be the ADC, that scatters the light originating on the pulsar (White & Holt 1982; Heinz & Nowak 2001; Iaria et al. 2013).

One possible scenario is that an extended Comptonizing region is in fact the accretion curtain as it falls towards the neutron star, and it is possible that the emission we see is actually produced by photons upscattered through this curtain. To investigate this more quantitatively, we build a toy model for the spectrum, in which the underlying emission from the star (which we assume to consist of a blackbody and Comptonized hard X-ray component) is upscattered by hot electrons in the infalling accretion curtain. We use the method and code of D'Angelo et al. (2008) to produce the final Compton upscattered spectrum. We start with an initial input spectrum (assumed originating from the stellar surface) of a blackbody plus an additional power-law component with a cutoff at high energies. We then use this as a seed photon spectrum to generate an output spectrum as a result of inverse Compton upscattering through a hot (e.g. $\gtrsim$ 10keV) thermal electron cloud.

To model this process we use a Monte Carlo Compton scattering code, whose details are described in Giannios & Spruit (2004). Briefly, the code works by using the seed photon spectrum as the initial photon energy distribution, and then calculating the outcome (final photon energy and direction) of a seed photon inverse Compton scattering off a hot electron. The electron cloud energy distribution is assumed to be thermal, and the temperature of the cloud is an input parameter of the simulation. The cloud is assumed to be isotropically surrounding the source of seed photons, and the probability of scattering depends mainly on the optical depth of the electron cloud (another input parameter).

The model thus has six free parameters, four for the input spectrum: the blackbody temperature ($t_{\rm bb}$), the power-law slope (Γ) and cut-off energy (E_c), the relative strength of the blackbody to power law (N), and two for the Comptonizing cloud: its temperature (T_e) and optical depth (τ). We vary these parameters in order to explore the range of temperatures and optical depths for the electron cloud that could be made consistent with the observed X-ray spectrum.

The requirement of an ADC has been introduced in the literature to explain the excess of light seen during the eclipses, with the X-ray flux never reaching a

value of zero as expected from a full eclipse. The X-ray flux is seen hovering at around 50% of its non-eclipse value. Furthermore the very long duration of the partial eclipses (about 80% of the orbit) requires an extended source surrounding the central X-ray source (White & Holt 1982; Hellier et al. 1990). The ADC was suggested to be formed from evaporated material in the accretion disk (White & Holt 1982). Shakura & Sunyaev (1973) suggested that the central source of X-ray binaries could evaporate material from the disk, and that if the material does not escape the system, it could form a corona-like cloud around the central source. White & Holt (1982) showed that the central source is always obscured if the inclination angle of the system is more than 60°, which is compatible with what is observed for 2A 1822-371, with an inclination angle of $i = 82.5° \pm 1.5°$ (Heinz & Nowak 2001). As we have shown in section 2.3.4 this scenario is compatible with the behaviour of the pulsed fraction as a function of the orbital phase. Indeed the fractional amplitude of the pulsations is consistent with being constant regardless of the orbital phase of the binary. This implies that the neutron star is obscured by some material throughout the orbit. Another important point is that the fractional amplitude of the pulsar does not vary with the depth of the eclipses. This does support the idea that the surface of the neutron star is never observed and that the pulsations we do see are indeed scattered through some medium, e.g., an ADC or an accretion stream.

Iaria et al. (2001, 2015) and Parmar et al. (2000) previously suggested that the ADC must be optically thick. This was also discussed by Heinz & Nowak (2001), and Iaria et al. (2013), who stated that an optically thick ADC is not consistent with the pulsations observed. To explore the possibilities for a lower value for the optical depth we explored the parameter space for the optical depth, the power law index and the electron temperature of the Compton up-scattering cloud. We found it possible to create an input spectrum, that, sent through the Compton up-scattering cloud, would be similar to the fitted spectrum with a high optical depth used by Iaria et al. (2015). This can be seen on Fig. 2.6, where the red line is the fit used by Iaria et al. (2015), the blue line is the input spectrum we created, using both a power law and a black body, and the black line is the output spectrum after the input spectrum has been sent through a Compton cloud.

The blue line on Fig. 2.6 corresponds to a power law index of $\Gamma = 1$, electron temperature of $E_c = 10$keV and optical depth of $\tau = 1$. Our test of the optical depth should be taken only as a proof of principle, that a model spectra with a black body and a power law can recreate the spectra observed *even if the optical depth is small*. The quality of the spectra and its match with the spectra found for example by Iaria et al. (2015) is judged by eye and by the normalized root mean square deviation which we find to be 28%.

The limits for the electron temperature is $3 < T_e < 15\,\mathrm{keV}$, the power law index limits are $0.5 < \Gamma < 1.5$ and the acceptable range of optical depth is $0.01 < \tau < 3$. Within these limits the spectra are reasonably reproduced with a much lower optical depth that is thus compatible with the presence of pulsation without requirement an optically thick Comptonization region plus an optically thick scattering ADC as suggested in Iaria et al. (2013). These results are also

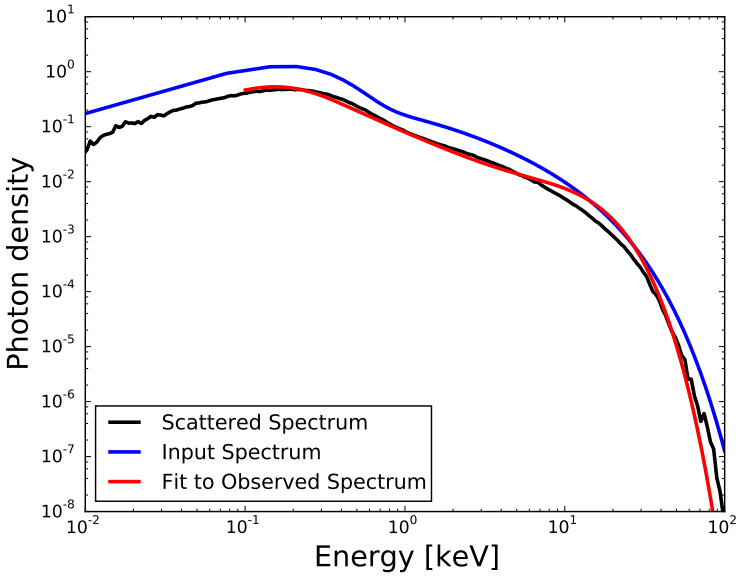

Figure 2.6: The black line represents the best simulated spectrum. The black line is our guess corresponding to the red line, which is the fit to the spectrum of 2A 1822-371 used by Iaria et al. (2015). The blue line is the input spectrum we have used, consisting of both a black body and a power law component.

compatible with recent spectral modelling performed by Niu et al. (2016) which discussed the possibility that the accretion disk corona around 2A 1822-371 is indeed optically thin.

The fit we created give a simple structure of the system, where the ADC is surrounding the pulsar, and reaching further out than the secondary star, making the pulsar light coming from an extended source, and thus both explaining the pulsations and the 50% depth of the eclipses. The structure of the system we suggest is initially very simple when compared to what White & Holt (1982) suggested. By analysing a spectrum that consists of both a power law and black body component, it is possible to eliminate the optically thick Comptonizing region, and thus explain the system only with an optically thin (or moderately thick; $\tau \approx 0.01 - 3$) ADC surrounding the pulsar. Another possibility for the geometry is that we could be seeing this system through an extended accretion stream. This stream scatters the light and pulsations just as an ADC would do. Assuming this as an explanation, simplifies the structure of the system even further.

2A 1822-371 is not the only suggested ADC systems. Another such system is MS 1603.3+2600. MS 1603.3+2600 was discovered by Morris et al. (1990) and has a 1.7 hr orbital period (Jonker et al. 2003b). The source shows both similarities and differences with 2A 1822-371. Both sources appear to be at a fairly high inclination, although the precise value for the inclination angle is not known for

MS 1603.3+2600. MS 1603.3+2600 is thought to be at a distance of about 6–24 kpc (Parmar et al. 2000; Jonker et al. 2003b; Hakala et al. 2005). Despite not showing accretion powered pulsations, MS 1603.3+2600 has a neutron star primary, since the source shows type I X-ray bursts (Jonker et al. 2003b; Hakala et al. 2005). The existence of an ADC around the source is supported by variations in the X-ray bursts. Hakala et al. (2005) looked at two XMM-*Newton* observations taken on 2003 January 20 and 22. They observed several Type I X-ray burst candidates. The bursts during the first observation have a count rate of about 6 counts s^{-1} whereas those seen during the second part of the observation only have a count rate of 2-3 counts s^{-1}. The variation suggests that the bursts are not directly observed, thus it is possibly only scattered X-rays that are observed, with the scattering medium forming an ADC (Hakala et al. 2005).

2.4.4 2A 1822-371 as a super Eddington source

A big weakness of the model that we have discussed so far is that it requires an Eddington limited accretion rate, despite the binary containing a low mass main sequence star that should transfer mass at a rate of about 10^{-10} $M_\odot$ yr^{-1}. Jonker et al. (2003a) performed detailed optical observations of 2A 1822-371 and suggested that one possible interpretation of the spectroscopic results is that the donor star is out of thermal equilibrium. Cowley et al. (2003) also suggested that the donor must be somewhat evolved since otherwise it would not fill its Roche lobe. Muñoz-Darias et al. (2005) also proposed that 2A 1822-371 is a LMXB which descends from an intermediate mass X-ray binary progenitor (initial $M \gtrsim 1\,M_\odot$), with the companion that has already lost a substantial amount of mass. In this case the mass transfer would not be driven by angular momentum loss via magnetic braking and/or gravitational radiation but would proceed on the thermal (Kelvin-Helmotz, KH) timescale of the companion (see e.g., King et al. 1996).

The thermal timescale is $\tau_{KH} \approx GM_2^2/(2R\,L_{nucl})$ where G is the universal gravitational constant, M_2 is the companion mass, R_2 its radius and L_{nucl} the nuclear stellar luminosity. The stellar luminosity is not well known in 2A 1822-371 since the optical observations are usually dominated by the disk emission/irradiation. Furthermore, as shown by King et al. (1995), the thermal timescale changes when irradiation is present, since the stellar surface luminosity might exceed the nuclear luminosity. Since the observed X-ray luminosity is of the order of 10^{36} erg s^{-1} and assuming that all the irradiation luminosity is re-emitted by the stellar surface of the donor, the irradiation luminosity would, due to geometric effects, correspond to approximately 10^{34} erg s^{-1} and the KH timescale becomes $\tau_{KH} \gtrsim 10^7$ yr, using M_2=0.46 $M_\odot$ and R_2 corresponding to the Roche lobe radius, R_L=0.6 $R_\odot$. If the companion star evolved on the τ_{KH} timescale, then the mass transfer rate can be as high as $\sim 10^{-7}$ $M_\odot$ yr^{-1}

We now try to interpret the observations of 2A 1822-371 in light of this hypothesis. In the following there is a big uncertainty on most parameters, thus the results could vary within an order of magnitude, and are only approximate. The orbital separation of 2A 1822-371 changes for two reasons: 1. the redistribution of angular momentum in the binary and 2. the loss of angular momentum via

magnetic braking/gravitational wave emission (see e.g., Frank et al. (2002)):

$$\frac{\dot{a}}{a} = \frac{2\dot{J}}{J} + \frac{-2\dot{M}_2}{M_2}(1-q) \tag{2.7}$$

here $q = M_2/M_{\rm NS}$ is the mass ratio between the companion (M_2) and neutron star mass ($M_{\rm NS}$), a is the orbital separation, J is the angular momentum and the dot refers to the first time derivative. In J we include all effects, e.g. magnetic breaking, gravitational waves and mass loss (Tauris & van den Heuvel 2006). If the mass transfer $\dot{M}_2 \approx 10^{-7}\, M_\odot\, yr^{-1}$ then, assuming to first order a conservative mass transfer scenario ($\dot{J} \approx 0$) we expect a relative variation of the orbit $\dot{a}/a \sim 10^{-14}\, s^{-1}$. The observations of the orbital period derivative $\dot{P}_{\rm orb} \approx 1.51 \times 10^{-10}$ (Iaria et al. 2011) provide a direct test of this hypothesis. Indeed from the 3-rd Kepler law we expect that $\dot{a}/a = 2\dot{P}_{\rm orb}/3P_{\rm orb}$ and the observed values give: $2\dot{P}_{\rm orb}/3P_{\rm orb} \approx 5 \times 10^{-15}\,{\rm s}^{-1}$ which is in good agreement with the hypothesis that 2A 1822-371 is evolving on a thermal timescale in a conservative mass transfer scenario.

Since the mass transfer is super-Eddington we can follow the line of reasoning of King & Lasota (2016), where they examine the case of the Ultra-Luminous X-ray source (ULX) M82 X-1. If that donor in M82 X-1 is in a super-Eddington mass transfer phase then the mass accretion rate, magnetic radius and the magnetic moment of the neutron star (μ) can be inferred from first principles. We argue here that one remarkable possibility to explain the phenomenology of 2A 1822-371 is that it is a mildly super-Eddington source.

In this case the accretion disk will be the standard Shakura-Sunyaev geometrically thin disk down to the so-called spherization radius (Shakura & Sunyaev 1973):

$$R_{\rm sph} = \frac{27}{4}\frac{\dot{M}_{\rm tr}}{\dot{M}_{\rm Edd}} R_{\rm g} \tag{2.8}$$

where $\dot{M}_{\rm tr}$ and $\dot{M}_{\rm Edd}$ are the mass transfer rate ($10^{-7}\,{\rm M}_\odot\,{\rm yr}^{-1}$) and the Eddington limit for a neutron star (that we set equal to $\approx 2 \times 10^{-8}\,{\rm M}_\odot\,{\rm yr}^{-1}$) and the $R_{\rm g} = GM/c^2 \approx 2 \times 10^5\,{\rm cm}$ is the neutron star gravitational radius ($M_1 = 1.69\,{\rm M}_\odot$). This gives a spherization radius of $\sim 10^7$ cm. Beyond this radius the flow will become geometrically thick and generate a funnel flow that can produce beaming (see e.g., King (2009)).

If the innermost region of the accretion disk is truncated at the magnetospheric radius $R_{\rm M}$, with $R_{\rm M} < R_{\rm sph}$, then the local mass accretion rate in any annulus of the disc with radius $R < R_{\rm sph}$ needs to be:

$$\dot{M}(R) = R/R_{\rm M}\dot{M}_{\rm Edd}. \tag{2.9}$$

Together with the expression for the magnetic dipole moment and spin up (Eq. 2.6), the spherization radius and the mass accretion rate equations (Eq. 2.8, 2.9) form a set of 4 equations with four variables, $R_{\rm sph}$, $\dot{M}(R_{\rm M})$, μ and $R_{\rm M}$. Following the method by King & Lasota (2016) one finds $R_{\rm M} \sim 10^6 - 10^7$ cm, $\mu \approx 1 \times 10^{28}\,{\rm G\,cm}^3$ (corresponding to a magnetic field of $\approx 2 \times 10^{10}\,{\rm G}$ at the poles and assuming a

$\dot{M}(R_{\rm M}) \approx 2 \times 10^{-8}\,{\rm M}_\odot\,{\rm yr}^{-1}$). The fact that the spherization radius and the magnetospheric radius are very close suggests that only the innermost portions of the accretion disk must be geometrically thick and generate a strong outflow. Such outflow might be responsible for the observed ADC since it will surround the central X-ray source. The value of the magnetic field is somewhat smaller than the one inferred from the possible cyclotron line reported by Iaria et al. (2015) although it is of the same order of magnitude despite the large uncertainties involved. Indeed we suggest that:

- The donor star of 2A 1822-371 is irradiated by a luminosity of $\approx 10^{36}\,{\rm erg\,s}^{-1}$.
- The irradiation drives a thermal timescale mass transfer of the order of $10^{-7}\,{\rm M}_\odot\,{\rm yr}^{-1}$.
- The super-Eddington mass transfer rate generates an outflow at the spherization radius, very close to the magnetospheric radius.
- The inner regions of the disk are geometrically thick and obscure the central source, as seen in Fig. 2.7.

Since the donor (and the observer) are nearly parallel to the accretion disk plane, even a very mild beaming will be sufficient to direct most of the radiation outside the line of sight of both the donor and the observer. Therefore the donor will not be irradiated by an X-ray luminosity much larger than the observed $L_{\rm X} \approx 10^{36}\,{\rm erg\,s}^{-1}$.

Finally, as a self-consistency check we need to verify whether the angular momentum loss due to the expulsion of material from the Roche lobe of the neutron star can alter significantly the orbit of the binary. As a limiting case we assume that all the material transferred in the neutron star Roche lobe is expelled and thus, following Postnov & Yungelson (2006):

$$\frac{\dot{J}_{\rm orb}}{J_{\rm orb}} = \beta \frac{\dot{M}_2\, M_2}{M_{\rm NS} M_{\rm T}} \approx 10^{-16}\,{\rm s}^{-1} \tag{2.10}$$

where $M_{\rm T} = M_2 + M_{\rm NS}$ is the total binary mass (assumed here to be approximately $2\,{\rm M}_\odot$) and $J_{\rm orb}$ and $\dot{J}_{\rm orb}$ are the total orbital angular momentum of the binary and its variation, and β is the fraction of the mass that is expelled. By inserting this value in Eq. 2.7 and by considering that $\dot{M}_2 \approx 10^{-7}\,{\rm M}_\odot\ {\rm yr}^{-1}$ we see that the final value of $\dot{a}/a$ is still of the order of $10^{-14}\,{\rm s}^{-1}$ which, again, is compatible with the observations.

2.4.4.1 Possible Tests of the Proposed Model

If 2A 1822-371 is really a mildly super-Eddington source then:

- The neutron star magnetic field must be of the order of a few times 10^{10} G.
- The source should not show any torque reversal in the near future.
- An outflow from the neutron star must be present and possible radio emission from a jet/outflow should be expected.

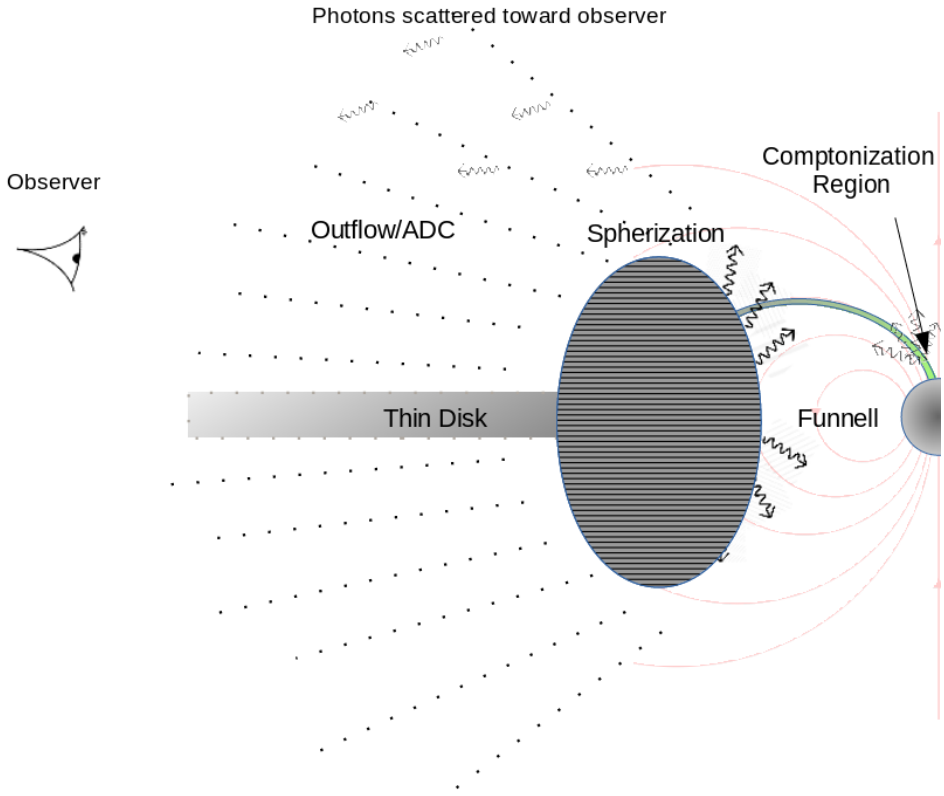

Figure 2.7: The illustrations show the geometry of the problem according to the super-Eddington scenario that we propose for 2A 1822-371 . The observer is located at an inclination angle $i = 82°$ and we have chosen an aligned rotator for simplicity. The thick part of the accretion disk begins at the spherization radius and ends at the magnetospheric radius where the plasma becomes channeled towards the neutron star poles. The accretion flow along the magnetic field lines is abruptly stopped a the neutron star surface and a shock forms close to the neutron star surface. It is in this shock that the Comptonization process takes place. The outflow generates instead an optically thin cloud around the neutron star that is responsible for the scattering of a small portion of the X-ray photons towards the direction of the observer.

2.5 Conclusion

We examined 13 years of data from *RXTE*, and conclude that the long-term spin frequency derivative and the two phase connected data sets, where we found short-term spin frequency derivatives, support an overall fast spin-up. The spin-up supports previous work by Jain et al. (2010); Iaria et al. (2015) and Chou et al. (2016). We tested if there was any flux-phase correlation present in this pulsar as there is in other systems, but found that there were no correlation.

We propose that the 2A 1822-371 is a relatively young binary (age of $\sim 1 - 10\,\mathrm{Myr}$) in which the donor is in a thermal timescale mass transfer phase. The orbital variation observed can be explained by the effect of the redistribution of angular momentum in the binary with no need for a large mass outflow from the donor star. An outflow is instead expected from the Roche lobe of the neutron star as a consequence of the nearly Eddington mass accretion rate occurring close to the neutron star magnetospheric radius. We propose that the outflow generates a large scale optically thin corona with $\tau \approx 1$ that surrounds the system. The lack of variability in the fractional amplitude suggests however, that the central source is always partially obscured and thus an optically thick region must form close to the neutron star at the approximate location of the spherization radius. We propose that this optically thick region generates a mild beaming as a consequence of the super-Eddington mass transfer rate. The Eddington/super-Eddington luminosity is not seen directly since the observer is viewing the source nearly edge on, in a way similar to what happens in the black hole binary SS433 (King 2009).

Bibliography

Aly J. J., 1985, A&A, 143, 19
Bayless A. J., Robinson E. L., Hynes R. I., Ashcraft T. A., Cornell M. E., 2010, ApJ, 709, 251
Beri A., Jain C., Paul B., Raichur H., 2014, MNRAS, 439, 1940
Bhattacharya D., van den Heuvel E. P. J., 1991, Phys. Rep., 203, 1
Bildsten L., et al., 1997, ApJS, 113, 367
Bradt H. V., Rothschild R. E., Swank J. H., 1993, A&A, 97, 355
Burderi L., Di Salvo T., Riggio A., Papitto A., Iaria R., D'Aì A., Menna M. T., 2010, A&A, 515, A44
Cavecchi Y., et al., 2011, ApJ, 740, L8
Chakrabarty D., et al., 1997, ApJ, 474, 414
Chou Y., Hsieh H.-E., Hu C.-P., Yang T.-C., Su Y.-H., 2016, preprint, (arXiv:1608.04190)
Cowley A. P., Schmidtke P. C., Hutchings J. B., Crampton D., 2003, AJ, 125, 2163
D'Angelo C. R., Spruit H. C., 2010, MNRAS, 406, 1208
D'Angelo C. R., Spruit H. C., 2012, MNRAS, 420, 416
D'Angelo C., Giannios D., Dullemond C., Spruit H., 2008, A&A, 488, 441
Frank J., King A., Raine D. J., 2002, Accretion Power in Astrophysics: Third Edition
Ghosh P., Lamb F. K., 1979, ApJ, 234, 296
Giacconi R., Murray S., Gursky H., Kellogg E., Schreier E., Tananbaum H., 1972, ApJ, 178, 281
Giannios D., Spruit H. C., 2004, A&A, 427, 251
Goodson A. P., Winglee R. M., Böhm K.-H., 1997, ApJ, 489, 199
Griffiths R. E., Gursky H., Schwartz D. A., Schwarz J., Bradt H., Doxsey R. E., Charles P. A., Thorstensen J. R., 1978, Nature, 276, 247
Hakala P., Ramsay G., Muhli P., Charles P., Hannikainen D., Mukai K., Vilhu O., 2005, MNRAS, 356, 1133
Harlaftis E. T., Charles P. A., Horne K., 1997, MNRAS, 285, 673
Hartman J. M., et al., 2008, ApJ, 675, 1468
Haskell B., Patruno A., 2011, ApJ, 738, L14
Heinz S., Nowak M. A., 2001, MNRAS, 320, 249
Hellier C., Mason K. O., Smale A. P., Kilkenny D., 1990, MNRAS, 244, 39P
Iaria R., Di Salvo T., Burderi L., Robba N. R., 2001, ApJ, 557, 24
Iaria R., di Salvo T., Burderi L., D'Aí A., Papitto A., Riggio A., Robba N. R., 2011, A&A, 534, A85
Iaria R., Di Salvo T., D'Aì A., Burderi L., Mineo T., Riggio A., Papitto A., Robba N. R., 2013, A&A, 549, A33
Iaria R., et al., 2015, A&A, 577, A63
Jahoda K., Markwardt C. B., Radeva Y., Rots A. H., Stark M. J., Swank J. H.,

Strohmayer T. E., Zhang W., 2006, ApJs, 163, 401
Jain C., Paul B., Dutta A., 2010, MNRAS, 409, 755
Ji L., Schulz N. S., Nowak M. A., Canizares C. R., 2011, ApJ, 729, 102
Jonker P. G., van der Klis M., 2001, ApJL, 553, L43
Jonker P. G., van der Klis M., Groot P. J., 2003a, MNRAS, 339, 663
Jonker P. G., van der Klis M., Kouveliotou C., Méndez M., Lewin W. H. G., Belloni T., 2003b, MNRAS, 346, 684
King A. R., 2009, MNRAS, 393, L41
King A., Lasota J.-P., 2016, MNRAS, 458, L10
King A. R., Frank J., Kolb U., Ritter H., 1995, ApJ, 444, L37
King A. R., Frank J., Kolb U., Ritter H., 1996, ApJ, 467, 761
Lovelace R. V. E., Romanova M. M., Bisnovatyi-Kogan G. S., 1995, MNRAS, 275, 244
Maccarone T. J., Girard T. M., Casetti-Dinescu D. I., 2014, MNRAS, 440, 1626
Mason K. O., Cordova F. A., 1982, ApJ, 262, 253
Morris S. L., Liebert J., Stocke J. T., Gioia I. M., Schild R. E., Wolter A., 1990, ApJ, 365, 686
Muñoz-Darias T., Casares J., Martínez-Pais I. G., 2005, ApJ, 635, 502
Niu S., Yan S.-P., Lei S.-J., Nowak M. A., Schulz N. S., Ji L., 2016, Research in Astronomy and Astrophysics, 16, 57
Papitto A., D'Aì A., Motta S., Riggio A., Burderi L., di Salvo T., Belloni T., Iaria R., 2011, A&A, 526, L3
Parmar A. N., Oosterbroek T., Del Sordo S., Segreto A., Santangelo A., Dal Fiume D., Orlandini M., 2000, A&A, 356, 175
Patruno A., Wijnands R., van der Klis M., 2009, ApJ, 698, L60
Patruno A., Hartman J. M., Wijnands R., Chakrabarty D., van der Klis M., 2010, ApJ, 717, 1253
Patruno A., Alpar M. A., van der Klis M., van den Heuvel E. P. J., 2012a, ApJ, 752, 33
Patruno A., Alpar M. A., van der Klis M., van den Heuvel E. P. J., 2012b, ApJ, 752, 33
Podsiadlowski P., Rappaport S., Pfahl E. D., 2002, ApJ, 565, 1107
Postnov K. A., Yungelson L. R., 2006, Living Reviews in Relativity, 9, 6
Sasano M., Makishima K., Sakurai S., Zhang Z., Enoto T., 2014, PASJ, 66, 35
Shakura N. I., Sunyaev R. A., 1973, A&A, 24, 337
Somero A., Hakala P., Muhli P., Charles P., Vilhu O., 2012, A&A, 539, A111
Tauris T. M., van den Heuvel E. P. J., 2006, Formation and evolution of compact stellar X-ray sources. pp 623–665
Ustyugova G. V., Koldoba A. V., Romanova M. M., Lovelace R. V. E., 2006, ApJ, 646, 304
White N. E., Holt S. S., 1982, ApJ, 257, 318
White N. E., Becker R. H., Boldt E. A., Holt S. S., Serlemitsos P. J., Swank J. H., 1981, ApJ, 247, 994

Yi I., Wheeler J. C., Vishniac E. T., 1997, ApJ, 481, L51
van Straaten S., van der Klis M., Méndez M., 2003, ApJ, 596, 1155
van der Klis M., 2001, ApJ, 561, 943